

New Features in Kinetic Energy Distribution of Laser-Induced Si⁺ Desorption from Si(100)

H. T. Liu* and Z. Wu

Department of Physics, Rutgers University, Newark, New Jersey 07102
(Received 3 September 1993)

Silicon ion desorption from Si(100) under the irradiation of low fluence 193 nm pulsed laser beam is studied using high resolution mass-selected time-of-flight technique. New features in the kinetic energy distribution of desorbed Si ions have been observed. A simple model is used to calculate the kinetic energies of desorbed Si⁺, and reasonably good agreement with measured values is obtained.

PACS numbers: 79.20.Ds, 68.45.Da

Substrate particle desorption under the bombardment of photons and electrons has attracted much attention in recent years. Compared with metallically bonded surfaces [1] and ionically bonded surfaces [2], substrate particle desorption from covalently bonded surfaces is not as quantitatively understood [3–12]. Under the irradiation of high laser intensity ($\geq 5 \times 10^9$ W/cm²), substrate particle emission from silicon surfaces is believed to result from surface evaporation and plasma formation [5]. Desorption of Si⁺ from silicon surfaces under the irradiation of much lower laser intensity ($\sim 5 \times 10^6$ W/cm²) has also been reported [7], but the mechanism is not fully understood. Time-of-flight (TOF) technique was used to study the kinetic energy of emitted particles. The TOF spectrum of emitted Si neutrals, taken at relatively high laser intensity ($\geq 4 \times 10^7$ W/cm²), was found to consist of a broad peak, which shifts toward higher energy as laser fluence increases [4]. Because of low resolution in the ion detection system, the structure of the TOF spectra for lower laser intensity irradiation was not studied [8].

In this Letter we report the observation of new features in ion kinetic energy distribution of Si⁺ desorption from Si(100) under the irradiation of 193 nm pulsed laser beam (< 300 mJ/cm² or 1.7×10^7 W/cm²). To the best of our knowledge, these new features have not been reported before. In addition to providing insight into the desorption mechanism, these new features may also be useful in quantitative studies of laser-induced surface processes, e.g., surface premelting, the onset of laser-induced plasma, etc. A simple model based on the localization of two holes in the back bond of surface Si atoms is used to calculate the kinetic energy of desorbed Si⁺. The calculated energies are in reasonable agreement with the measured ones.

The experiment was carried out in an ultrahigh vacuum chamber with a base pressure 5×10^{-10} Torr. The Si(100) sample, 18 mm \times 5 mm \times 0.38 mm in size, was Czochralski grown (Wacker) and P-doped *n*-type with a resistivity of ~ 5 Ω cm. The sample was cleaned by 2 keV Ar⁺ sputtering, annealing at 925 K and flashing to 1400 K for 30 s [13]. The cleanliness of the sample was confirmed by an Auger spectrometer. The temperature of the sample was measured in the following way.

Two identical Si(100) samples were clamped together by 0.002-in. molybdenum foil. A small dent was drilled on the back piece so that a 0.003-in. W-26%Re/W-5%Re thermocouple was snugly sandwiched between the two Si samples. Samples were heated by passing dc current through them. Only the front sample was used in the study. The 193 nm laser beam from an excimer laser (pulse width ~ 17 ns), after passing through an aperture of 5 mm diameter and a beam splitter, was focused by a lens ($f = 26$ cm) through a quartz window onto the sample and exited through another quartz window. The angle of incidence was 65°. Laser fluence was varied by changing the distance between the lens and the sample while keeping the laser power fixed. The typical beam size on the sample was 0.5 mm².

The desorbed Si ions were detected using mass-selected time-of-flight technique. A quadrupole mass analyzer (UTI 100C) was used to perform the mass selection. To avoid the background signal due to neutral residual gas molecules such as CO, the ionizer assembly in the analyzer was tuned off and grounded. The collection angle was 0.01 sr. The ion signal, after being amplified by a fast preamplifier, was recorded by a multichannel scaler (EG&G ORTEC T914) with the dwell time per channel being set to 70 ns. A fast silicon photodiode monitored the reflected laser light from the beam splitter and triggered the start (flight time = 0) of the multichannel scaler. The *z* component of the ion velocity is given by $v_z = L/t$, where *z* is the sample surface normal, which also coincides with the axis of the mass filter, *L* is the flight length (22 cm), and *t* is the flight time.

Shown in Figs. 1(a) and 1(b) are, respectively, the representative raw TOF data for various laser fluences and the corresponding kinetic energy distributions as obtained from the TOF spectra: $dN/dE_k = (t^3/mL)dN/dt$, where *N* is the number of ion counts and *m* the ion mass. All the spectra were taken on grounded samples at 300 K. For laser fluence lower than 150 mJ/cm², four peaks centered at 56, 48, 41, and 32 μ s, which correspond respectively to 2.2, 3.0, 4.2, and 6.9 eV, are observed. Each peak seems to contain subpeaks, the origin of which is unknown. As laser fluence increases, the peak positions remain approximately the same, in contrast to the TOF spectra

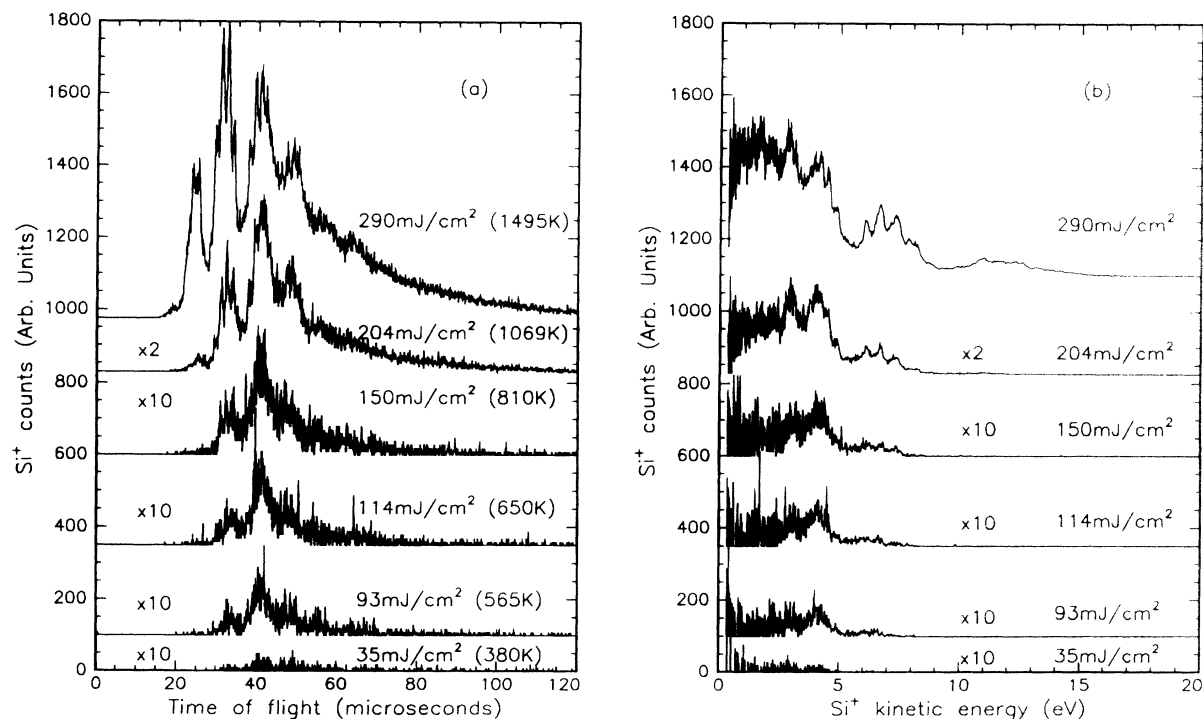


FIG. 1. (a) Representative raw TOF data desorbed Si ions for various laser fluences. Each TOF spectrum is the accumulation of 1000 laser shots. The laser fluence is calculated from $P/\pi r^2$, where P is the measured power (J) and r the $1/e$ beam radius as measured using a small ($10 \mu\text{m}$ diameter) pinhole. Therefore, assuming a Gaussian distribution for the fluence, the indicated fluence represents peak fluence at the center of the irradiated spot. Estimated temperature at the center of the spot due to laser heating [14] is indicated for each laser fluence. (b) The corresponding ion kinetic energy distribution.

of emitted Si neutrals under the irradiation of higher laser fluence [4]. For fluence higher than 150 mJ/cm^2 , a peak at $25 \mu\text{s}$ (11.3 eV) begins to develop and its position shifts toward higher energy as laser fluence increases. This 11.3 eV peak can also be seen for lower laser fluence if the substrate is resistively heated to sufficiently high temperature (e.g., 1200 K). Thus it seems that the 11.3 eV peak is related to laser-induced thermal or plasma excitation. The nature of this peak is not fully understood.

It should be mentioned that the rather dramatic features in the TOF spectra of desorbed Si ions can only be observed for relatively low laser fluence. At high fluence ($>400 \text{ mJ/cm}^2$), the lower energy peaks start to merge together to form a broad featureless peak, which we interpret as the onset of surface premelting and will be discussed in more detail elsewhere.

The location of various peaks in the TOF spectra shown in Fig. 1 is characteristic (i.e., very reproducible experimentally) of a clean Si(100) surface, independent of sample cleaning procedures (e.g., Ar^+ sputtering followed by annealing and flashing vs annealing and flashing only). However, ion counts vary from sample to sample and also depend on sample cleaning procedures. Therefore, unlike the kinetic energy of desorbed Si^+ , so far we have not been able to obtain reproducible data of Si^+ yield. It is observed on all samples, however,

that the dependence of ion counts on laser fluence can be described by two different power laws. A representative plot of fluence dependence is shown in Fig. 2. Nonlinear fluence dependence of integrated ion yield has been reported for both Si^+ [5–7] and Ga^0 desorption [10]. It is interesting to point out that the turning point (150 mJ/cm^2) at which the power law changes corresponds to the appearance of the 11.3 eV peak in the kinetic energy distribution. This observation has not been reported before.

In attempting to understand the new features in the TOF spectra we have considered various possibilities, including both surface and gas phase excitations [15]. For example, the signal may be due to CO^+ or Si^+ ionized in the gas phase. However, the results of the following controlled experiments argue that the observed signal is due to surface electronic excitation. (1) Features similar to those in Fig. 1 are also observed on Si(100) surface resistively heated to 1200 K , a temperature at which there should be no adsorbed species such as CO [16]. (2) Consider the possibility that the observed signal is due to gas phase ionization of desorbed CO. For a base pressure of $5 \times 10^{-10} \text{ Torr}$ and a laser repetition rate of 5 Hz , one can estimate that the number density of gaseous CO above the sample during laser pulse is $<4 \times 10^{13}/\text{cm}^3$ or 10^{-3} Torr . No signals were observed when the chamber

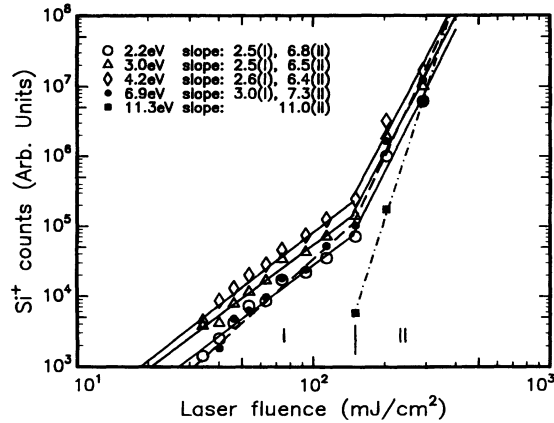


FIG. 2. A representative plot of the laser fluence dependence of Si ion counts corresponding to each energy peak in the TOF spectra. The ion counts are normalized to fluence per unit area of illumination.

was filled with up to 4 Torr of CO (99.99% purity) and the sample moved away from the laser beam. (3) The two-photon ionization probability of a gaseous Si atom by the laser pulse is $\sigma_2 I^2 \tau$, where $\sigma_2 \approx 10^{-50} \text{ cm}^4 \text{ s}$ is the two-photon ionization cross section [17], I the laser intensity in photons per cm^2 per s, and τ the laser pulse width. Thus, even for the highest laser fluence used in this study, the ionization probability is $< 5 \times 10^{-8}$, 2 orders of magnitude lower than the electron-impact ionization probability in the ionizer assembly. Therefore, if the observed Si^+ signal is due to gas phase ionization of desorbed neutral Si atoms, the neutral Si signal should be about 2 orders of magnitude larger than the Si^+ signal. By turning on the filament in the ionizer and positively biasing a grid in front of the ionizer, one can measure the TOF spectrum of desorbed Si neutrals. For the laser fluence used in this study, the Si neutral signal, if any, is not detectable within the featureless background TOF spectrum, and is estimated to be at least 1 or 2 orders of magnitude smaller than the Si^+ signal. Therefore we conclude that the observed Si^+ signal is not due to gas phase ionization of desorbed neutral Si atoms. (4) When the distance between the sample and the mass analyzer was varied, the flight time was found to scale with the flight length correctly. This rules out the possibility that the signal may originate from other surfaces, e.g., inner surfaces of the quadrupole analyzer due to scattered laser light.

As a first attempt to understand the kinetic energy distribution of Si ions, we use the following model, which, though oversimplified, seems to account for the main features in the TOF spectra. The model makes three assumptions: (1) Si ions desorb from singly bonded surface Si atoms, e.g., adatoms; (2) Si ions desorb in their ground electronic states [18]; and (3) desorption of a Si ion results from the localization of two holes in the back bond (i.e., the *removal* of the back bond) of

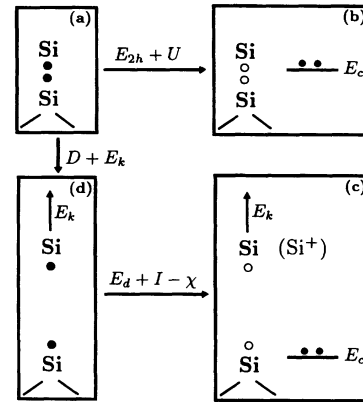


FIG. 3. A singly bonded Si atom just before (b) and right after (c) its desorption as Si^+ . The open circles in (b) represent localized holes in the back bond surface state. The open circle on the substrate Si atom in (c) represents a hole in the dangling bond and that on the departing Si atom indicates a missing electron, i.e., a Si^+ . The filled holes in (b) and (c) represent electrons at the bottom of the conduction band.

a surface Si atom [11, 19]. A localized two-hole state can live sufficiently long for desorption to occur when the Coulombic repulsion between the two holes is greater than the width of the band to which the two holes belong [20]. Therefore one would expect this mechanism to be more effective at surface defect sites where the bands are narrower. We will estimate the kinetic energy E_k of Si^+ using an argument similar to that used in the Hess law in physical chemistry. As a first order approximation, the back bond and dangling bond energies as calculated in Ref. [21] will be used for the singly bonded Si surface atoms. The configurations just before and right after desorption are depicted in Figs. 3(b) and 3(c). The main electronic relaxation processes during desorption are (1) the hole left on the surface Si atom becomes a dangling bond hole and (2) the hole on the departing Si atom corresponds to ionization of the Si atom. Therefore if we assign the dangling bond energy to the hole left on the surface Si atom and ionization energy to the departing Si atom in Fig. 3(c), the configurations (b) and (c) will have approximately the same energy. The configuration (b) can be obtained from (a) by providing energy $E_{2h} + U$, where E_{2h} is the energy required to excite two electrons

TABLE I. Kinetic energy E_k of desorbed Si^+ .

Surface states:	E (eV) ^a	E_{2h} (eV)	E_k (eV) [from Eq. (1)]	E_k (eV) (obs.)
P_3 at K point:	-2.6	7.4	1.6	2.2
P_2 at K point:	-3.2	8.6	2.8	3.0
P_1 at K point:	-3.7	9.6	3.8	4.2
S_5 at K point:	-5.9	14.0	8.2	6.9

^aReference [21].

from the back bond to the bottom of the conduction band in the absence of screened hole-hole repulsion U . The energy needed to convert (a) to (c) is $D + E_k + E_d + I - \chi$, where $D = 1.8$ eV is the Si-Si bond energy [22], E_d is the energy required for exciting an electron from the surface dangling bond to the bottom of the conduction band, $I = 8.18$ eV is the ionization energy of a Si atom, and $\chi = 4.0$ eV is the electron affinity of silicon [23]. By equating the energies of (b) and (c), we get

$$E_k = E_{2h} + U - D - E_d - I + \chi. \quad (1)$$

Therefore in this model the different energy peaks in Fig. 1 correspond to different back bond surface states from which localized two-hole states are created. Localized two-hole states are created by multiphoton excitation, leading to a nonlinear dependence of the ion yield on laser fluence. Since U is not known, we use U as an adjustable parameter to fit the observed energy peaks. The values of E_k calculated from Eq. (1) using the values of E_{2h} and E_d (1.9 eV) from Ref. [21] are shown in Table I together with the observed values. The best fit requires $U = 2.1$ eV. This is smaller than the value of $U \sim 8-10$ eV in the Si-H bond [19], indicating that screening is larger in the Si-Si bond than in the Si-H bond.

This work is supported by NSF Grant No. DMR-9022134.

*Permanent address: Department of Physics, University of Science and Technology of China, Hefei, Anhui, China.

- [1] W. Hoheisel *et al.*, Phys. Rev. Lett. **60**, 1649 (1988); H.S. Kim *et al.*, in *Desorption Induced by Electronic Transitions, DIET V*, edited by A.R. Burns, D.R. Jennison, and E.B. Stechel (Springer-Verlag, Berlin, 1993), p. 95.
- [2] M. Knotek and P. Feibelman, Phys. Rev. Lett. **40**, 964 (1978); M. Szymonski, in *Desorption Induced by Electronic Transitions, DIET IV*, edited by G. Betz and P. Varga (Springer-Verlag, Berlin, 1990), p. 270, and references therein.
- [3] For a review on DIET on covalently bonded surfaces, see D.E. Ramaker, in *Desorption Induced by Electronic Transitions, DIET I*, edited by N. Tolc *et al.* (Springer-Verlag, Berlin, 1990), p. 70.
- [4] B. Stritzker *et al.*, Phys. Rev. Lett. **47**, 356 (1981); A. Pospieszczyk *et al.*, J. Appl. Phys. **54**, 3176 (1983).
- [5] J.M. Liu *et al.*, in *Laser and Electron-Beam Interactions with Solids*, edited by B.R. Appleton and G.K. Celler (Elsevier, New York, 1982), p. 29.
- [6] J.M. Moison and M. Bensoussan, J. Vac. Sci. Technol. **21**, 315 (1982).
- [7] L. Chen *et al.*, J. Vac. Sci. Technol. A **6**, 1426 (1988).
- [8] L. Chen (private communication).
- [9] T. Nakayama, Surf. Sci. **133**, 101 (1983).
- [10] K. Hattori *et al.*, Phys. Rev. B **45**, 8424 (1992); J. Kanasaki *et al.*, Phys. Rev. Lett. **70**, 2495 (1993).
- [11] N. Itoh and T. Nakayama, Phys. Lett. **92A**, 471 (1982); N. Itoh *et al.*, Phys. Lett. **108A**, 480 (1985).
- [12] Z. Wu, in *Desorption Induced by Electronic Transitions, DIET IV* (Ref. [2]), p. 163.
- [13] C.C. Cheng and J.T. Yates, Phys. Rev. B **43**, 4041 (1991); C.C. Cheng *et al.*, J. Appl. Phys. **67**, 3693 (1990).
- [14] H.S. Carslaw and J.C. Jaeger, *Conduction of Heat in Solids* (Oxford Univ. Press, Oxford, 1986), 2nd ed., p. 75. Since quantities such as specific heat, thermal conductivity, etc., are functions of temperature [B.G. Koehler and S.M. George, Surf. Sci. **248**, 158 (1991)], a self-consistent calculation was carried out to estimate the temperature rise.
- [15] The importance of gas phase ionization in DIET was studied by R.E. Walkup *et al.*, Phys. Rev. B **36**, 4577 (1987).
- [16] B.A. Joyce and J.H. Neave, Surf. Sci. **34**, 401 (1973); H.F. Dylla *et al.*, Surf. Sci. **74**, 141 (1978).
- [17] G. Mainfray and C. Manus, in *Multiphoton Ionization of Atoms*, edited by S.L. Chin and P. Lambropoulos (Academic, New York, 1984), p. 10.
- [18] This assumption does not hold for gas phase processes, where fragment ions can be produced in excited states from dissociation of excited doubly ionized molecular ions. See N. Saito and I.H. Suzuki, J. Chem. Phys. **91**, 5329 (1989); M. Larsson *et al.*, J. Phys. B **23**, 1175 (1990).
- [19] H.H. Madden *et al.*, Phys. Rev. B **26**, 896 (1982).
- [20] M. Cini, Solid State Commun. **24**, 681 (1977); G.A. Sawatzky, Phys. Rev. Lett. **39**, 504 (1977); P. Feibelman, Surf. Sci. **102**, L51 (1981); D.R. Jennison *et al.*, Phys. Rev. B **25**, 1384 (1982).
- [21] M. Schmeits *et al.*, Phys. Rev. B **27**, 5012 (1983).
- [22] L. Pauling, *The Nature of The Chemical Bond* (Cornell Univ. Press, New York, 1960), 3rd ed., p. 85.
- [23] R.M. Broudy, Phys. Rev. B **1**, 3430 (1970).